Electronic structure evolution during the growth of ultra-thin insulator films on semiconductors: from interface formation to bulk-like CaF_2/Si(111) films.

Andreas Klust,[1,*] Taisuke Ohta,[2,†] Aaron A. Bostwick,[1,†] Eli Rotenberg,[3] Qiuming Yu,[1] Fumio S. Ohuchi,[2] and Marjorie A. Olmstead[1]

[1] *University of Washington, Department of Physics, Box 351560, Seattle, WA 98195, USA*
[2] *University of Washington, Department of Materials Science and Engineering, Box 352120, Seattle, WA 98195, USA*
[3] *Advanced Light Source, Lawrence Berkeley National Laboratory, Berkeley, CA 94720, USA.*

(Dated: October 19, 2005)

The electronic structure of ultra-thin (0.3-6 nm) epitaxial insulator films grown on semiconductors, represented by the prototypical system CaF_2/Si(111), was studied using scanning tunneling spectroscopy (STS) and photoemission spectroscopy (PES). The surface states related to the (7×7) reconstruction of the substrate are completely removed during the formation of the interface and an interface state is established in the CaF_2 band-gap close to the Fermi level. While the band-gap of CaF_2 films only two molecular layers thick is essentially bulk-like, a film thickness of about 3 nm is necessary to fully develop the bulk CaF_2 valence band structure.

PACS numbers:
Keywords: electronic properties, insulator films, CaF_2/Si(111)

I. INTRODUCTION

The development of the electronic band structure of films ranging from (sub-)monolayers to the fully developed bulk band structure is important for understanding the electronic properties of nanostructures. Most studies published so far concentrated on metal films grown on metal substrates (e.g. Cr/Au(100)[1], Gd/W(110)[2] or Ni/Cu(100)[3]) or semiconductor films grown on semiconductor substrates (e.g. GaAs/AlAs(100)[5]). Insulating films received considerably less attention, probably due to the experimental problems resulting from charging effects.

Emerging applications in nanotechnology require structures composed from different classes of materials such as metals, semiconductors, and insulators. For instance, many modern device structures such as resonant tunneling diodes (RTDs) consist of several different materials in layers that are each only few atomic layers thick.[6,7] Tunneling barriers require wide-band-gap layers with well-known electronic properties, where the barrier thickness must be controlled to the monolayer level due to the exponential dependence of tunneling currents on the barrier thickness. With tunneling barrier thicknesses in the range of a single nm (3-4 molecular layers), a single extra atomic layer would drastically reduce the tunneling current, while a single missing layer can create unacceptable leakage currents. Such ultra-thin films consist essentially only of interfaces to the surrounding materials, raising the question of whether the ad-hoc assumption of bulk materials properties is at all valid. In this paper, we present a layer-resolved study of the electronic properties of ultra-thin insulator films grown on semiconductors represented by the prototypical system CaF_2/Si. We address the question if and how electronic properties of these films deviate from their bulk material properties.

The electronic properties of thin films can be assessed by a wide range of experimental techniques such as photoemission spectroscopy, x-ray absorption spectroscopy, and optical absorption and emission measurements. All these techniques, however, average over a relatively large sample area. Although all these techniques are in principle able to measure properties of a film that is only one molecular layer thick, layer resolved measurements are often restricted by inhomogeneous film morphologies within the measurement area. Scanning tunneling spectroscopy, however, allows measurement of electronic structures with high spatial resolution and surface sensitivity.

Although scanning tunneling microscopy (STM) and spectroscopy (STS) are restricted to conductive samples, insulating films grown on conductive substrates can be examined if the film thickness is thin enough to prevent charging.[8] For instance, electrons can be injected from the STM tip into the insulator's conduction band using a sufficiently high positive sample bias voltage. These electrons are conducted through the insulating film into the conductive substrate if the insulator film thickness does not exceed the electron mean free path at the conduction band minimum of the insulator. Electrons trapped in the insulator can also contribute to the conduction through the insulator film although it is probably not enough to achieve stable imaging conditions for STM.

The thickness dependent electronic properties of an ultra-thin insulator film grown on a metal substrate has been determined by Schintke et al. using layer-resolved STS for the case of MgO on Ag(100).[9] They found that a MgO film with only 3 molecular layers thickness already has the bulk band-gap. In this paper, we present layer-resolved STS measurements of the electronic properties of an ultra-thin insulator film epitaxially grown on

a semiconducting substrate. In addition to STS, we employed photoemission spectroscopy (PES) to study the development of the valence band with increasing CaF_2 film thickness. We use epitaxial CaF_2 films grown on Si(111) as model system for this investigation because the interface between CaF_2 and Si is well characterized and atomically smooth CaF_2 films can be grown on Si.[10]

CaF_2 is an ionic material with a large band-gap of 12 eV. The small lattice misfit with Si of 0.6% at room temperature makes it a promising material for epitaxial growth.[10,11] The structure of the interface between CaF_2 and Si(111) has been thoroughly investigated using many different experimental methods such as x-ray photoelectron spectroscopy[12,13] and diffraction[14–16], x-ray diffraction[17,18], medium energy ion scattering[19], and x-ray standing waves[20,21]. The most stable interface configuration is given by a bilayer with CaF stoichiometry that is overgrown by bulk-like CaF_2.[10] In the CaF bilayer, one layer Ca binding to the Si substrate is terminated by a single F layer.

II. EXPERIMENTAL CONSIDERATIONS

Both sample preparation for the STS experiments and STM measurements were carried out in the same commercial ultra-high vacuum (UHV) STM system.[22] Si samples cut from a boron doped wafer were annealed at about 600 °C for >12 h in UHV before flash annealing for 10 s at about 1300 °C to remove the native oxide layer. The quality of the clean Si(111)-(7×7) reconstruction was checked using low-energy electron diffraction and STM. CaF_2 was sublimed from a Knudsen cell. The deposition rate of 0.3-0.6 triple layer (TL)/min (one TL corresponds to one layer of Ca atoms embedded between two layers of F and contains $7.8{\cdot}10^{14}$ molecules/cm^2) was controlled using a quartz microbalance. The resulting coverage was determined with STM. About 1.2 TL CaF_2 were deposited at sample temperatures of 640 °C measured with an infrared pyrometer. After growth at these conditions, the Si substrate is completely covered with the CaF bilayer. The additional 0.2 TL CaF_2 form islands on top of the CaF bilayer. All STM and STS measurements were done at room temperature.

Photoemission spectroscopy measurements were done at beamline 7.0.1.2 of the Advanced Light Source (ALS) at the Lawrence Berkeley National Laboratory (LBNL). During sample growth at the ALS, the first 3 TL CaF_2 were deposited at ∼650 °C to produce a well ordered CaF/Si interface[15] resulting in the Si substrate covered by the CaF bilayer with the remaining 2 TL CaF_2 forming islands on top of the CaF bilayer. The remainder of the film was deposited at ∼450 °C to minimize the strain in the CaF_2 and to promote flat film growth. The growth rate in both cases was 1-2 TL/min as determined by a quartz microbalance. The microbalance gives reliable information on the CaF_2 amount deposited at 450 °C because the CaF_2 sticking coefficient is close to unity at temperatures below ∼600 °C. The films were grown as a wedge of graded thickness from 0 to 25 TL, by moving a shutter in front of the sample during growth. The small x-ray beam diameter of 50 μm allowed for taking photoemission spectra at different spots of the sample that correspond to different film thicknesses. The photons were incident at an angle of ∼60° to the sample normal with p-polarization. To minimize the effects of photostimulated desorption of fluorine from the CaF_2[23], the sample was moved 0.1 mm (twice the nominal beam diameter) between successive spectra. The photon exposure was chosen such that no noticeable changes were seen if two spectra were taken in the same place. The binding energy is referred to the Fermi-level position which was determined by measuring the Fermi-level position of the metallic sample holder.

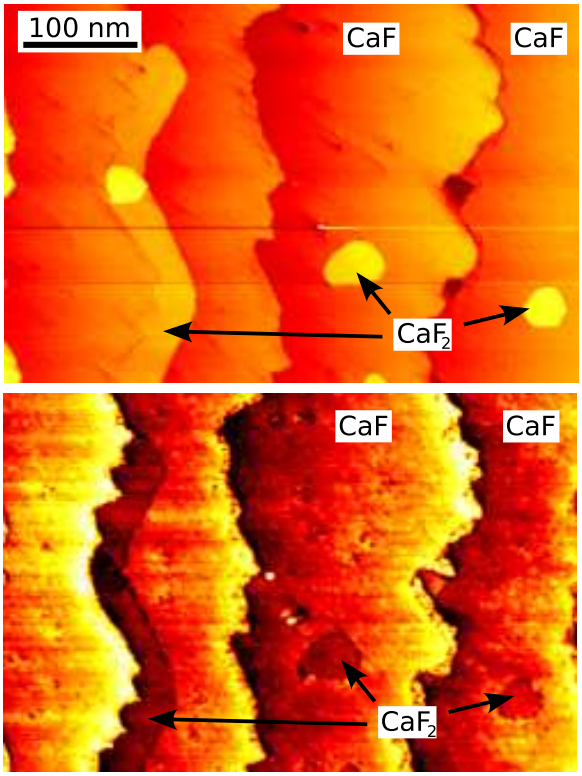

FIG. 1: (Color online) STM images of the CaF_2 film taken with 100 pA tunneling current and bias voltages of +3.5 V (top) and -9.0 V (bottom). The film consists of the CaF bilayer with an additional ∼0.2 TL CaF_2 in islands on top of it. CaF bilayer terminated terraces and CaF_2 islands are marked in the image. The two CaF_2 islands at the lower right corner of the image are imaged as protrusions in the positive bias image and as depression in the negative bias image.

At the growth temperatures used here, the interface between the CaF_2 and the Si substrate consists of a single CaF bilayer.[12,13,15,16,19,21] During growth, the CaF bilayer completely covers the Si substrate before the growth of stoichiometric CaF_2 on top of it starts.[24] On stepped

substrates like the ones used here, step edges act as barriers for the growth of the CaF_2.[25]

The contrast in STM images of CaF_2 films depends strongly on the bias voltage (Fig. 1). A positive bias voltage of +3.5 V is high enough for electrons to tunnel from the tip into the CaF_2 conduction band. Therefore, STM images obtained with this voltage reflect the sample topography. For negative bias voltages of -9.0 V, however, the image contrast is reversed. CaF_2 islands grown on the CaF bilayer are imaged as depressions.[26] This contrast inversion was used to distinguish CaF_2 islands from the CaF bilayer for the STS experiments presented here.

STS spectra were acquired on a grid while imaging in constant current mode: every 5th scanline scanning was interrupted for every 5th point. The feedback loop was disabled and the tunneling current was acquired while linearly varying the bias voltage at a constant tip-sample distance. All STS spectra shown below are averages of at least 50 spectra taken with the same parameters at different positions on the same sample. STS data obtained using different tips and samples were consistent with the data shown below.

It has been demonstrated previously that the normalized conductivity $(dI/dV)/(I/V)$ provides a measure for the local density of states.[27] On samples with a band-gap, however, the ratio I/V approaches zero faster than the ratio dI/dV. Therefore, $(dI/dV)/(I/V)$ tends to diverge at the band edges. To avoid this problem, we artificially broadened the I/V curve before computing $(dI/dV)/(I/V)$, using a least-square fit of an exponential function to the measured I/V curve instead of I/V to normalize dI/dV.[28] This extreme broadening of I/V avoids the divergence of the normalized conductivity at the band edges. The derivative dI/dV was computed numerically. The tunneling current drops below the noise level of the tunneling current amplifier within the band-gap of the sample. This results in a high noise level in the computed dI/dV, which is amplified by computing the normalized conductivity. Therefore, we do not show data acquired in within the sample's band-gap except in the case of the (7×7) reconstructed Si(111) surface which has a sufficient density of states in the band-gap to avoid this problem.

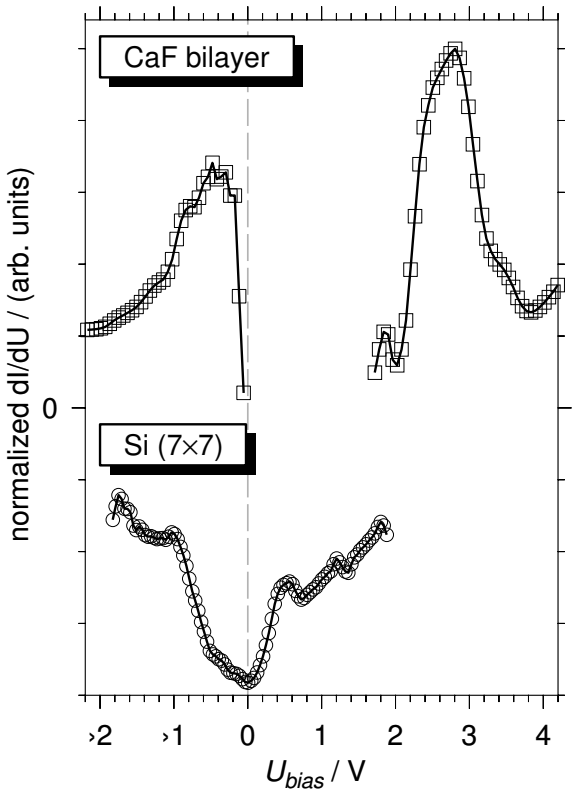

FIG. 2: STS spectra of the clean Si(111)-(7×7) substrate (bottom) and the CaF bilayer (top).

III. RESULTS AND DISCUSSION

The electronic structure of the surface changes drastically with the growth of the CaF bilayer (Fig. 2). The averaged STS spectrum taken on the Si substrate shows occupied states in the band-gap that are consistent with the metallic properties of the (7×7) surface reconstruction. The Fermi-level is located about 0.5 eV below the conduction band minimum (CBM) as expected for a (7×7) reconstructed Si(111) surface.[29] The (7×7) reconstruction of the Si substrate is removed during the growth of the CaF bilayer and the surface becomes non-metallic. The Fermi-level of the CaF bilayer is pinned at the valence band maximum (VBM) as found previously by photoemission spectroscopy and near-edge x-ray absorption experiments.[30]

The STS spectrum of the CaF bilayer (see Fig. 2) exhibits two pronounced peaks: One located 0.4 eV below the Fermi-level and the second 2.6 eV above the Fermi-level. The peak located 0.4 eV below the Fermi-level can be attributed to an interface state originating from the interaction of Ca 4s electrons with 3p dangling bond orbitals of the Si(111) surface. This is consistent with observations of the Si-Ca interface state by, e.g., angle-resolved photoelectron spectroscopy 0.8 eV below the Fermi-level at the surface Γ point.[31] We attribute the peak at 2.6 eV above the Fermi-level to the conduction band edge. Nonlinear optical measurements found a value of 2.4 eV for the interface band-gap.[32] This value for the interface band-gap agrees well with the difference between the onsets of the normalized (dI/dV) signal observed around the Fermi-level for the valence band and around 2.4 eV for the conduction band.

The surface electronic structure is changed further when a single molecular layer of CaF_2 is grown on the CaF bilayer (Fig. 3). The biggest difference can be seen at the VBM. The strong peak corresponding to the interface state 0.4 eV below the Fermi-level observed on the CaF bilayer is suppressed on the CaF_2 island. Al-

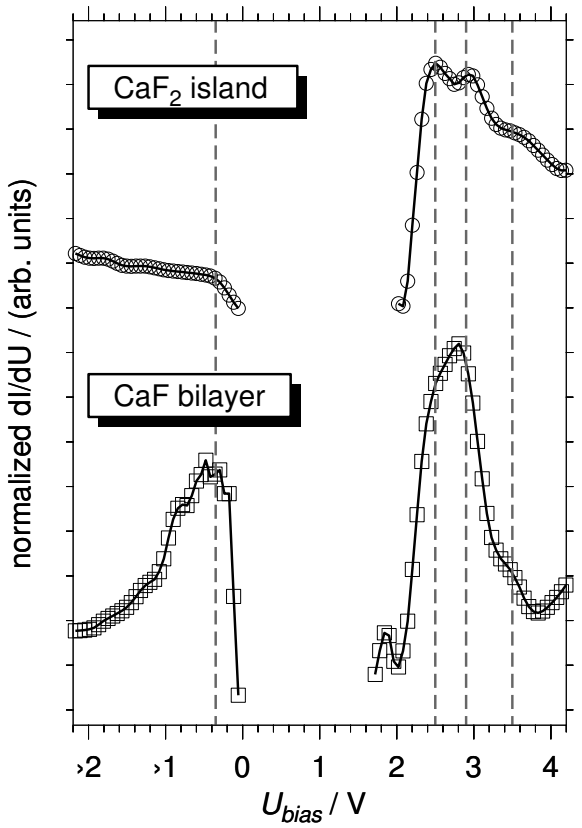

FIG. 3: Comparison between averaged STS spectra obtained on the CaF bilayer (bottom) and on a 1 molecular layer thick CaF_2 island grown on top of the CaF bilayer (top).

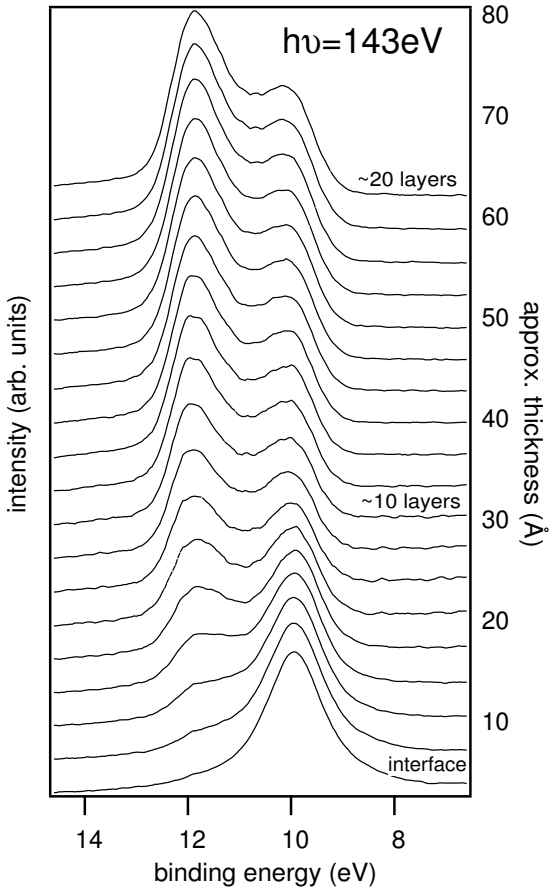

FIG. 4: Photoemission spectroscopy spectra taken at normal emission from a "wedge shape" CaF_2/Si film. The spectra were taken at positions with different film thickness.

though an onset can be seen around 0.4 eV below the Fermi-level, there is no peak visible in the spectrum for the CaF_2 island. This behavior is consistent with the assumption that the peak 0.4 eV below the Fermi-level corresponds to a state localized at the interface that is exponentially damped in the adjacent layers.

Previously published STS data on the CaF bilayer by Avouris and Wolkov showed the highest occupied states peak at 1.3 eV below and the lowest unoccupied states peak 1.2 eV above the Fermi-level.[8] The whole spectrum is shifted downwards by 0.9 eV with respect to our data. This shift can be explained by the use of n-type Si substrates in the study of Avouris and Wolkow as opposed to p-type substrates in our case. A more recent study of the conduction band edges of the CaF bilayer and CaF_2 with STS found the onset of the conduction band for the CaF bilayer and CaF_2 at 2.3 eV and 3.7 eV, respectively.[33] The authors attribute the onset at 2.3 eV above the Fermi-level to the conduction band minimum of the Si substrate in [111] direction rather than to the CaF bilayer.[33] This contradicts our findings that the conduction band onset of the CaF bilayer is essentially at the same position as the conduction band onset of single-layer CaF_2 islands. Photoemission spectroscopy studies show that the valence band offset between CaF_2 and Si depends on the exact growth conditions[13], which may explain the differences between the published STS data. Our main conclusions, however, are not influenced by the exact positions of the VBM and CBM. It should be noted that the detailed interpretation of STS data obtained for insulator/semiconductor heterostructures is complicated by the influence of various effects such as the ballistic transport through the insulator, scattering at the interface, and injection into Si bulk states in addition to the tunneling process from the tip into the CaF_2 film. This may explain why remnants of the interface state just below the Fermi-level are visible in the STS data obtained on the CaF_2 islands while the Si conduction band edge is absent in the STS spectra on both the CaF bilayer and the CaF_2 islands.

We used photoemission spectroscopy to study the development of the CaF_2 valence band with increasing film thickness (Fig. 4). The photon energy of 143 eV was chosen to achieve photoemission from states close to the Γ point of the bulk CaF_2 Brilloin zone, where two F 2p states (Γ_{15} and Γ'_{25}) are predicted from theoretical

calculations.[34] The PES results show that the F 2p derived valence band is not fully developed for films thinner than about 10 TL. The position of the upper edge of the CaF_2 valence band located 9.9 eV below the Fermi-level, however, is independent of the film thickness. The lower energy peak located 12 eV below the Fermi level is visible with the nucleation of the first CaF_2 layer, and its position is unchanged with thickness. However, the intensity of this peak (its matrix element) is not fully established until about 10 TL. Since this peak is derived from an odd parity (Γ'_{25}) state, the full selection rules are not established until the mirror symmetries are fully developed.[35] The position of the highest F 2p (Γ_{15}) state determined by photoemission and the CaF_2 bulk band-gap of 12.4 eV lead to an expected position of the conduction band edge at 2.5 eV above the Fermi-level. This value is consistent with the observation of the first conduction band peak in the STS spectra taken on CaF_2 islands at 2.5 eV.

IV. CONCLUSIONS

The combined STS and PES results show that although the main features of the CaF_2 band-structure develop quickly within the first two molecular layers, thicker films are needed to fully develop the CaF_2 bulk band structure. The surface states related to the Si(111)-(7×7) reconstruction are completely removed by the formation of the CaF_2/Si interface during the growth of the CaF bilayer. They are replaced with interface states associated with the bonds between Si and Ca[31] that pin the Fermi-level close to the valence band edge.

The bulk CaF_2 band structure develops starting with the first CaF_2 (triple)layer grown on top of the CaF. Both our STS and PES measurements indicate that an only two layer thick insulator film (CaF bilayer plus one CaF_2 layer) is enough to obtain the band-gap and valence band width at the Γ point of bulk CaF_2. An examination of the CaF_2 valence band formed by F 2p states with PES, however, suggests that a film thickness of about 10 TL is necessary to fully develop the matrix elements of the CaF_2 valence band, in particular the Γ'_{25} state requiring the development of mirror symmetries between different layers of F.

V. ACKNOWLEDGEMENTS

This work is supported by the U.S. Department of Energy grant no. DE-FG03-97ER45646 and the M. J. Murdock Charitable Fund. A.K. further gratefully acknowledges support by the Alexander von Humboldt-Foundation and T.O. financial support by the University Initiative fund of the University of Washington. We further gratefully acknowledge the support of the ALS staff while performing experiments at the Advanced Light Source, Lawrence Berkeley National Laboratory, which is operated by the U.S. Department of Energy under contract no. DE-AC03-76SF00098.

---

* Electronic address: klust@fas.harvard.edu; Present address: Department of Chemical Engineering, Stanford University, Stanford, CA 94305, USA

† Present address: Advanced Light Source, Lawrence Berkeley National Laboratory, Berkeley, CA 94720, USA.

[1] D. G. O'Neill and J. H. Weaver, Phys. Rev. B **37**, 8122 (1988).

[2] L. Dongqi, C. W. Hutchings, P. A. Dowben, W. Rong-Tzong, C. Hwang, M. Onellion, A. B. Andrews, and J. L. Erskine, J. Appl. Phys. **70**, 6565 (1991).

[3] C. Pampuch, O. Rader, R. Klasges, and C. Carbone, Phys. Rev. B **63**, 153409 (2001).

[4] T.-C. Chiang, Surf. Sci. Rep. **39**, 181 (2000).

[5] H. Asklund, L. Ilver, J. Kanski, S. Mankefors, U. Sodervall, and J. Sadowski, Phys. Rev. B **63**, 195314 (2001).

[6] T. Suemasu, M. Watanabe, J. Suzuki, Y. Kohno, M. Asada, and N. Suzuki, Jpn. J. Appl. Phys. **33**, 57 (1994).

[7] C. Strahberger and P. Vogl, Phys. Rev. B **62**, 7289 (2000).

[8] P. Avouris and R. Wolkow, Appl. Phys. Lett. **55**, 1074 (1989).

[9] S. Schintke, S. Messerli, M. Pivetta, F. Patthey, L. Libioulle, M. Stengel, A. D. Vita, and W.-D. Schneider, Phys. Rev. Lett. **87**, 276801 (2001).

[10] M. A. Olmstead, *Thin Films: Heteroepitaxial Systems* (World Scientific Publishing, Singapore, 1999), chap. Heteroepitaxy of Strongly Disparate Materials: From Chemisorption to Epitaxy in CaF_2/Si(111), pp. 211–266.

[11] L. J. Schowalter and R. W. Fathauer, CRC Critical Reviews in Solid State and Materials Science **15**, 367 (1989).

[12] F. J. Himpsel, U. O. Karlsson, J. F. Morar, D. Rieger, and J. A. Yarmoff, Phys. Rev. Lett. **56**, 1497 (1986).

[13] M. A. Olmstead, R. I. G. Uhrberg, R. D. Bringans, and R. Z. Bachrach, Phys. Rev. B **35**, 7526 (1987).

[14] J. D. Denlinger, E. Rotenberg, U. Hessinger, M. Leskovar, and M. A. Olmstead, Appl. Phys. Lett. **62**, 2057 (1993).

[15] J. D. Denlinger, E. Rotenberg, U. Hessinger, M. Leskovar, and M. A. Olmstead, Phys. Rev. B **51**, 5352 (1995).

[16] E. Rotenberg, J. D. Denlinger, M. Leskovar, U. Hessinger, and M. A. Olmstead, Phys. Rev. B **50**, 11052 (1994).

[17] C. A. Lucas, D. Loretto, and G. C. L. Wong, Phys. Rev. B **50**, 14340 (1994).

[18] K. G. Huang, J. Zegenhagen, J. M. Phillips, and J. R. Patel, Phys. Rev. Lett. **72**, 2430 (1994).

[19] R. M. Tromp and M. C. Reuter, Phys. Rev. Lett. **61**, 1756 (1988).

[20] J. Zegenhagen and J. R. Patel, Phys. Rev. B **41**, 5315 (1990).

[21] A. Klust, M. Bierkandt, J. Wollschläger, B. H. Müller, T. Schmidt, and J. Falta, Phys. Rev. B **65**, 193404 (2002).

[22] Omicron Nanotechnology GmbH, Taunusstein, Germany.

[23] V. Chakarian, T. D. Durbin, P. R. Varekamp, and J. A.

Yarmoff, Phys. Rev. B **48**, 18332 (1993).
[24] A. Klust, H. Pietsch, and J. Wollschläger, Appl. Phys. Lett. **73**, 1967 (1998).
[25] J. Wollschläger, Appl. Phys. A **75**, 155 (2002).
[26] A. Klust, T. Ohta, M. Bierkandt, C. Deiter, Q. Yu, J. Wollschläger, F. S. Ohuchi, and M. A. Olmstead, submitted for publication.
[27] N. D. Lang, Phys. Rev. B **34**, 5947 (1986).
[28] P. Martensson and R. M. Feenstra, Phys. Rev. B **39**, 7744 (1989).
[29] F. J. Himpsel, T. Fauster, and G. Hollinger, Surf. Sci. **132**, 22 (1983).
[30] D. Rieger, F. J. Himpsel, U. O. Karlsson, F. R. McFeely, J. F. Morar, and J. A. Yarmoff, Phys. Rev. B **34**, 7295 (1986).
[31] A. B. McLean and F. J. Himpsel, Phys. Rev. B **39**, 1457 (1989).
[32] T. F. Heinz, F. J. Himpsel, E. Palange, and E. Burstein, Phys. Rev. Lett. **63**, 644 (1989).
[33] J. Viernow, D. Y. Petrovykh, A. Kirakosian, J.-L. Lin, F. K. Men, M. Henzler, and F. J. Himpsel, Phys. Rev. B **59**, 10356 (1999).
[34] R. A. Heaton and C. C. Lin, Phys. Rev. B **22**, 3629 (1980).
[35] A. A. Bostwick, Ph.D. thesis, University of Washington, Seattle, USA (2004).